

# **Supplemental Materials**

***Molecular Biology of the Cell***

**Zaatri et al.**

**Supplement to Figure 2: Anterior-to-Posterior and binned velocities of septin loss of function cells**

(A-C) Mean and variance (+/- one standard deviation) of circumferential velocities over time averaged across the anterior-posterior axis. (D-I) Posterior-directed velocities over time for *unc-59(RNAi)*, *unc-59(e1005)*, and *unc-61(e228)* cells ( $n = 12$ ,  $n = 9$ ,  $n = 6$ , respectively). Gold, green, blue and dashed colored lines indicate individuals of the corresponding color-coded phenotype; black: septin perturbation population average; purple: control average. (G-I) Mean and variance (+/- one standard deviation) of posterior-directed velocities over time averaged across the top-bottom axis. (J-L) Binned circumferential velocities. Populations and color denotations are the same as panels D-F. (M-O) Binned posterior-directed velocities. Populations and color denotations are the same as panels D-F.

**Supplement to Figure 3: Controls for Figure 3**

(A) Mean intensity ratio (A/P) of UNC-59::GFP just prior to anaphase onset for control and *cyk-1(RNAi)* cells. Dots are individuals; horizontal bar is population mean; vertical notches are 95% confidence interval; ns = not significantly different. (B-F) Photobleaching adjustment for CYK-1::GFP cells. (B) Averaged fluorescence intensity CYK-1::GFP in cells treated with azide ( $n=10$ ) (B-C) Cortical fluorescence intensities over time in CYK-1::GFP control (C,  $n = 12$ ) and UNC-59 depleted (D,  $n = 5$ ) cells. (E-F) Photobleaching-corrected CYK-1::GFP intensities for the same cells as in B and C. Movies were recorded on the same settings as those made to build the decay model in (B); the decay coefficient was used to calculate and add in the intensity that was lost to photobleaching.

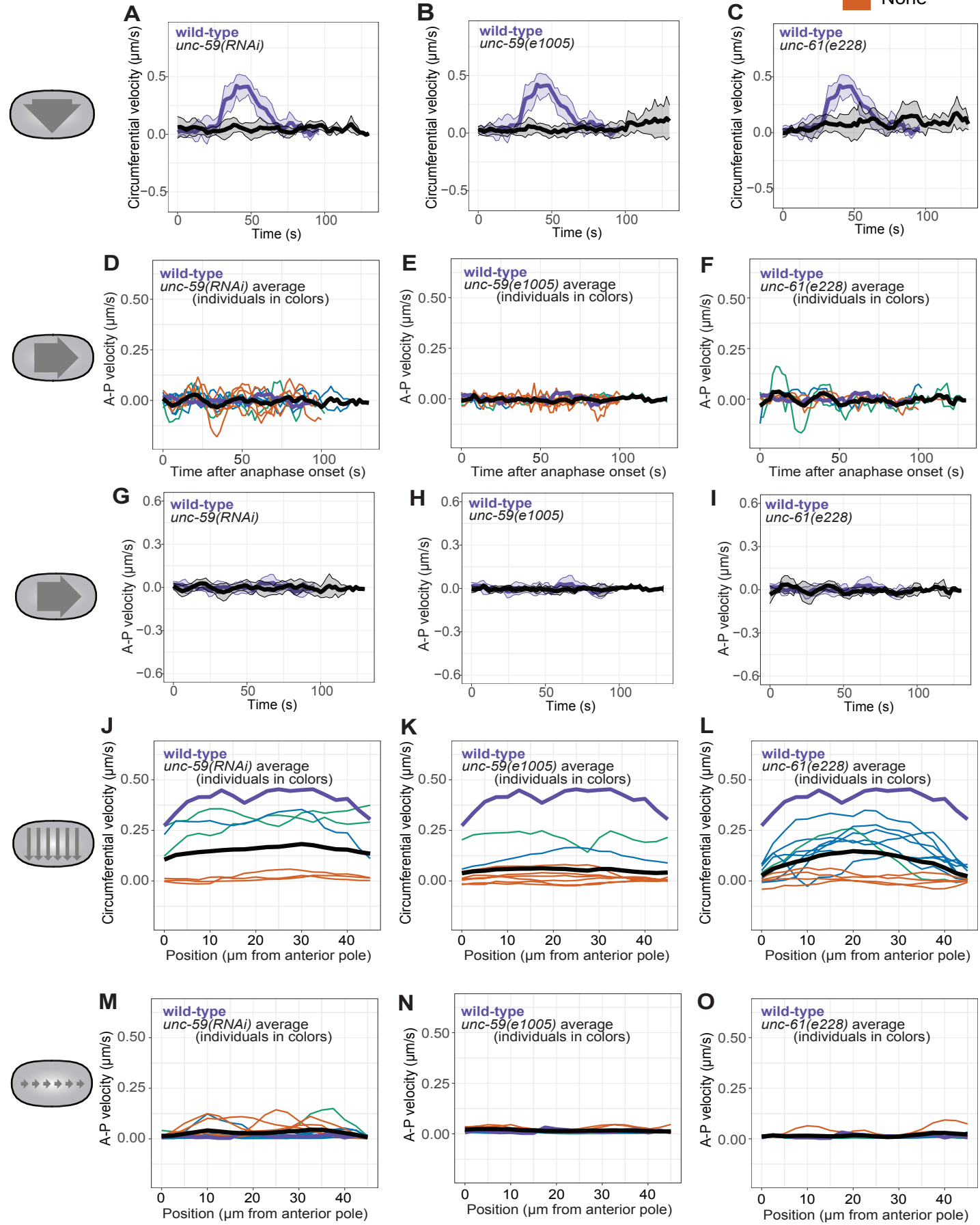
**Supplement to Figure 4: AP and binned velocities for CYK-1 loss of function cells**

(A and B) Mean and variance (+/- one standard deviation) of circumferential velocities over time averaged across the anterior-posterior axis. (C-F) Posterior-directed velocities over time for *cyk-1(RNAi)* and (*cyk-1(RNAi)*; *unc-61(e228)*) populations ( $n = 10$ ,  $n = 18$ ). Brown: (*cyk-1(RNAi)*; *unc-61(e228)*) population average; purple: wild-type average; red: *cyk-1(RNAi)* average. (C and D) Gold, green, blue and dashed colored lines indicate individuals of the corresponding color-coded phenotype. (E and F) Mean and variance (+/- one standard deviation) of posterior-directed velocities over time averaged across the top-bottom axis. (G and H) Binned circumferential velocities. Populations and color denotations are the same as panels A-B. Dashed line indicates reversed handedness. (I and J) Binned posterior-directed velocities. Populations and color denotations are the same as panels A-B.

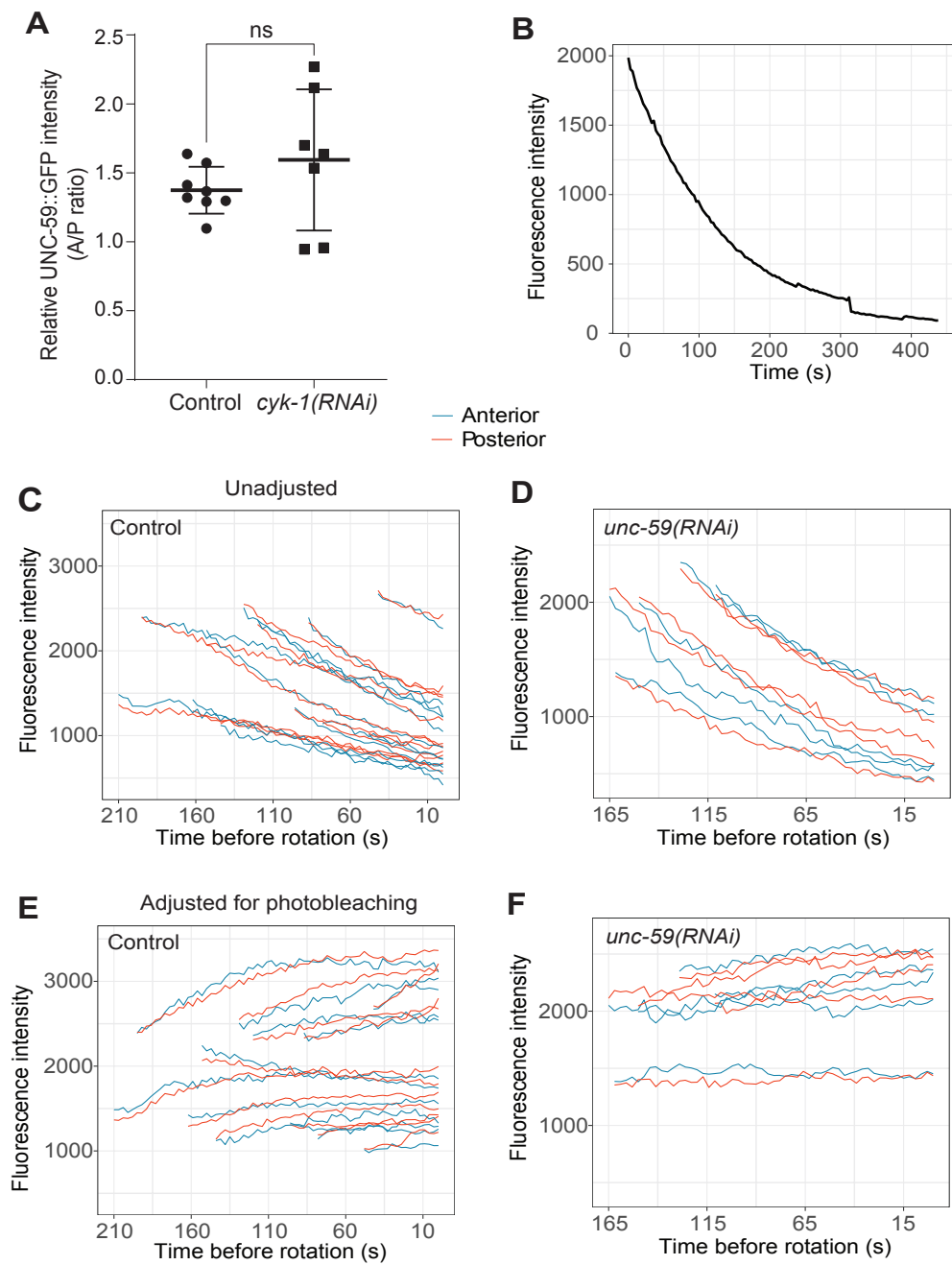
# Zaatri et al Figure 2 Supplement

**Rotation type**

- Continuous (Blue)
- Intermittent (Green)
- None (Orange)



# Zaatri et al Figure 3 Supplement



# Zaatri et al Figure 4 Supplement

**Rotation type:**

- [Yellow diagonal lines] Alternating handedness
- [Blue diagonal lines] Continuous, reversed handedness
- [Solid blue] Continuous
- [Solid green] Intermittent
- [Solid orange] None

